Proceedings of The Institute of Acoustics

APPLICATIONS OF PARAMETRIC ACOUSTIC ARRAYS IN LABORATORY SCALE EXPERIMENTS

V.F. Humphrey

School of Physics, University of Bath, Claverton Down, Bath,
BA2 7AY, England

ABSTRACT

The use of parametric acoustic arrays to make accurate experimental measurements in the laboratory is discussed and illustrated with examples. The wideband frequency ability and narrow beam cross-section characteristic of this type of source are shown and a typical experimental system described. The need to truncate the array to simplify the measurement procedure is also considered. The application of the source to the measurement of the transmission properties of limited size panels is described and illustrated with a range of experimental results. These show how the wideband nature of the source enables precise measurements to be made over an extended frequency range while the small spot size helps to reduce the significance of diffraction from the edges of the panel. The use of a parametric array to measure the backscattering from objects is also illustrated with a range of measurements on solid elastic spheres over the frequency range 10-175kHz.

INTRODUCTION

A parametric array uses the nonlinear propagation of primary wavefields to generate additional lower frequency components that are then used to make measurements. This type of source has two particular advantages. Firstly, the source produces a beam with a narrow cross-section and, secondly, the source may be operated over a wide range of frequencies. This paper illustrates how these advantages may be exploited to make carefully controlled acoustic measurements in the laboratory.

The principle of a parametric acoustic transmitting array was first proposed by Westervelt in 1960 [1] and demonstrated in practice soon afterwards [2]. Since then the theory and understanding of these sources has grown immensely and they have been used in a variety of sonar applications [3,4] and especially as sub-bottom profilers. Many laboratory experiments have been performed to gain a better understanding of the characteristics of this type of source and its use in sonar applications.

There are, however, other important applications for the parametric array in the laboratory, where it can be used as a very versatile acoustic source. In these situations the source is used because of its characteristic small spot size and its wideband frequency ability. In this paper the characteristics of parametric arrays that make them suitable for laboratory work will be described and the performance of a typical system will be illustrated. Two applications will be considered in detail: first, their use to measure the reflection and transmission loss of materials in the form of panels [5-7] and, second, their use to investigate the scattering properties of objects [8]. These examples will help to illustrate the advantages of this type of source for laboratory measurements.

LABORATORY APPLICATIONS OF PARAMETRIC ACOUSTIC ARRAYS

Parametric arrays have also been applied in the laboratory to general studies of scattering from rough surfaces [9]. Here the narrow beam cross-section enabled measurements to be made on surfaces without problems from edge diffraction, whilst the frequency ability enabled the scattering to be studied as the ratio of the acoustic wavelength to surface roughness was varied over a wide range. In addition the experiment was performed under carefully controlled conditions with the statistical properties of the surface known exactly. This type of application is currently being extended to studies of grazing incidence.

Other potential laboratory applications include the detailed study of edge diffraction from barriers or baffles of finite impedance and their use as a general acoustic source for hydrophone inter-comparisons. Preliminary work has indicated the potential of both these uses.

THE PARAMETRIC ARRAY

The basis of a parametric array is a conventional transducer which transmits high level primary waves into the water. These waves propagate in a nonlinear manner and as a result generate additional frequency components in the acoustic medium. These additional components, including the low frequency terms whose application is described here, can be considered to come from secondary sources distributed throughout the interaction region of the primary frequencies. The field produced by this distribution of sources can be evaluated by integrating over the source volume. It is the form and phasing of these "pseudo sources" that give the parametric array its narrow beam. The wideband nature of the source depends on the fact that the low frequency output can be simply changed by adjusting the primary frequencies within the bandwidth of the primary transducer.

Most of the work described here was performed by transmitting a short pulse of carrier (Figure 1(b)) with a "raised cosine bell" or "haversine" envelope (Figure 1(a)). For this type of transmission the low-frequency component of the parametric array output on axis can be shown [10] to be proportional to the second derivative, with respect to time, of the square of the transmitted pulse envelope. Thus the length and frequency content of the waveform generated can be adjusted by altering the frequency, f_c, of the sine wave used to generate the raised cosine bell envelope. A typical example of the lower frequency signal obtained in this way for f_c=40kHz is shown in Figure 1(c). The short low-frequency pulses obtained have a very wide bandwidth which makes them suitable for making measurements over a range of frequencies by Fourier analysis.

The spectrum of the output pulse shown in Figure 1(c) is shown in Figure 2. The shape of this spectrum, after allowing for the hydrophone response, is in good agreement with the theoretical prediction [10] with a -6dB bandwidth extending from 25kHz to 95kHz. Adjusting the length of the modulating envelope results in the demodulated pulse being extended or contracted in time with corresponding changes in the pulse spectrum. This is illustrated in Figure 2 which shows, to the same scale, the spectrum of the demodulated pulse obtained with an envelope based on 10kHz raised cosine bell. The resulting spectrum is now concentrated between 8 and 23kHz.

LABORATORY APPLICATIONS OF PARAMETRIC ACOUSTIC ARRAYS

THE EXPERIMENTAL SYSTEM

The results to be described were obtained using the electronic system shown in Figures 3 and 4 and described in detail in reference [6]. The pulse repetition frequency was controlled by a pulse generator which also triggered the transmitting and receiving electronics. The raised cosine bell produced by the function generator was used to amplitude modulate the carrier and the resulting pulse amplified and applied to a conventional transducer. This was 50mm in diameter, resonant at 920kHz and had a Q-factor of 5.8 that enabled a wide range of secondary frequencies to be efficiently generated.

The signals were received by a Brüel and Kjær 8103 hydrophone and passed through a passive low pass filter to ensure that no nonlinear intermodulation occurred in the subsequent electronics. The signals were then amplified and digitised (at 1MHz) with a signal processor. This also enabled the waveforms to be averaged over a number of "pings" to increase the signal to noise ratio and reduce the quantisation error. The resulting signals were then processed as necessary; the processing, including application of windows and FFTs, was performed by the processor and the signals stored on a computer.

All of the measurements to be described were performed in a test tank 1.2 x 1.2 x 1.8m in size without any acoustically absorbing lining material.

ARRAY TRUNCATION AND CHARACTERISTICS

In laboratory applications of the parametric array, such as those described here, the measurements are likely to be made in the nearfield of the transducer where the primary wave amplitudes are still high. This can give rise to two specific problems. Firstly, the measurement procedure may alter the primary wavefield and hence, the secondary source distribution. This complicates the measurement and makes it difficult to isolate the direct effect of the experiment on the secondary wavefield. Secondly, a number of workers have found [11-13] that significant errors can occur in measurements made in the presence of high amplitude primary waves due to the nonlinear response of some hydrophones.

It can, therefore, be advantageous to truncate the array with an acoustic filter that attenuates the high frequency primary waves while allowing the low frequency secondary waves to pass without significant loss. This produces a source free zone beyond the acoustic filter in which only the secondary frequencies of interest are present and where measurements can be made without these problems occurring.

Although it is possible to use a thin metallic sheet a quarter of a wavelength thick to reduce the amplitude of the transmitted primaries this does not have a very high differential transmission for primary and secondary frequencies. It is, therefore, better to use a material with higher absorption at the primary frequencies. In practice a sheet of cork-filled butyl rubber 13mm thick was used as the acoustic filter. This was acoustically well matched to water, had an insertion loss of 1.7dB at 100kHz and 42dB at 1MHz, and was suspended across the array at a distance L ($\approx$0.6m) from the transducer.

The truncation of the array alters the characteristics of the parametric beam, with the beam broadening beyond the acoustic filter. This is illustrated in Figure 5 which shows beam profiles for a frequency of 50kHz produced by an array truncated at 0.6m. The beam immediately beyond the filter shows the characteristic untruncated array beam pattern without sidelobes. However, at a range of 0.65 m the beam has already spread significantly with evidence of sidelobes starting to appear. Figure 6 shows beam cross-sections measured at a range of 0.1m from the acoustic filter for an array length of 0.56m. The results shown are for frequencies of 20kHz and 80kHz. The more rapid fall off of the higher frequency should be noted, as should the -6dB spot sizes of 0.23m at 20kHz and 0.11m at 80kHz. It is this small spot size that makes the parametric array a useful laboratory tool and makes it possible to make measurements without unwanted edge diffraction effects for example.

THE MEASUREMENT OF TRANSMISSION COEFFICIENTS

There is a requirement in underwater acoustics to be able to predict and measure experimentally the acoustic properties of materials in the form of plates immersed in water over a range of frequencies and for a range of angles of incidence. It can be important, for example, to know the amplitude and phase of the waves transmitted and reflected from a panel used as a window for a sonar system. Although it is possible to predict the response of isotropic panels using plane wave theory [14] if the elastic properties are known, experimental techniques are needed to confirm these predictions as materials are developed and to test non-isotropic and non-homogeneous materials. Impedance tube techniques may be used to make measurements at normal incidence but are not necessarily as convenient for oblique incidence or non-homogeneous materials due to the need to cut small samples.

An alternative method is to make freefield measurements using a conventional source. The insertion loss of a panel, for example, is often measured by recording the pressure produced by a source at a point with and without the panel present between the source and observation position. With conventional sources a number of transducers may be required to cover an extended frequency range and measurements on panels of limited size are complicated by diffraction from the edges of the panel, especially at lower frequencies.

Clearly a parametric source is ideally suited to this application as the small beam cross-section may be used to reduce the diffraction effects by minimising the insonification of the edges of the panel under test. In addition the wideband nature of the source enables the acoustic properties to be measured over a wide frequency range with only one transducer being required [5,6]. The results obtained with such an experimental technique are described below.

Normal Incidence Measurements.

The measurements of the transmission coefficient of a panel were made as follows. The parametric array was truncated at a range of about 0.6m and the hydrophone placed between 0.15m and 0.4m beyond the filter to receive the reference signal $f(t)$. The test panel was then inserted between the acoustic filter and the hydrophone, and the new signal $f_t(t)$ was recorded. The respective spectra $F(f)$ and $F_t(f)$ of these signals were calculated using an

FFT, and the experimental complex transmission coefficient $T'(f)$ calculated at each frequency from

$$T'(f) = F_t(f)/F(f) \quad . \tag{1}$$

Here the prime indicates that this is an amended transmission coefficient that differs from the normal definition [14] by an additional phase term corresponding to the time delay of the fluid path that is replaced by the panel. The modulus of this coefficient expressed on a decibel scale gives the insertion loss.

The experimental results for the insertion loss of an aluminium plate 10.7mm thick and 0.38 x 0.45m in size are shown in Figure 7 for normal incidence and the frequency range 10kHz to 120kHz. A very good agreement with the theoretical predictions of plane wave theory is observed with an agreement within 0.5dB. When making this type of measurement care must be taken to minimise multiple reflections between the test panel, acoustic filter and hydrophone. The ripple of 0.3dB on the experimental data in Figure 7 was attributed to a multiple reflection between the hydrophone and test panel.

Measurements like this showed that for acoustically thin panels the results obtained at normal incidence were in very good agreement with plane wave predictions [6]. However, measurements on acoustically thicker panels at both normal incidence and oblique incidence showed significant differences from plane wave theory [7]. These results were a consequence of the incident wavefield not being a plane wave.

The influence of the plane wave spectrum.

In order to calculate the influence of the acoustic field on measurements of insertion loss it is necessary to represent the field in terms of its plane wave spectrum and consider the effect of the panel under test on each component of the spectrum. The resulting field beyond the panel can then be evaluated by integrating over the plane wave spectrum. For the special case of a source with rotational symmetry the complex amplitude A(z) of the field at a point (0,0,z) on the axis of symmetry can be expressed [7] in the form

$$A(z) = ik \int_0^{\pi/2-i\infty} S(\theta)\, e^{ikz\cos\theta} \sin\theta \, d\theta, \tag{2}$$

where θ is measured from the symmetry axis and $S(\theta)$, the plane wave spectrum, is a function of θ only. It is now necessary to consider the effect of inserting an infinite panel of thickness d between the source and observation point, normal to the z axis (the axis of symmetry). For an isotropic panel in this situation the transmission coefficent $T'(\theta)$ will be a function of θ only. The transmitted wavefield, $A_t(z)$, at the same field point can therefore be written in the form

$$A_t(z) = ik \int_0^{\pi/2 - i\infty} S(\theta)\, T'(\theta)\, e^{ikz\cos\theta} \sin\theta \, d\theta, \qquad (3)$$

where $T'(\theta)$ is the amended plane wave transmission coefficient for a wave incident at an angle θ to the normal. The exponential term in the integrand of equation (3) produces very rapidly fluctuating real and imaginary parts with variations in θ for large values of kz, except in the vicinity of the "stationary phase point", $\theta=0$. If the plane wave spectrum is taken into account it may be concluded that the most significant contribution to the integral comes from the region where θ is small. Hence if the transmission coefficient varies slowly with angle for small values of θ then it may be replaced by its value for $\theta=0$ and taken outside the integral to give

$$A_t(z) = T'(0)\, A(z) \qquad (4)$$

and the experimental transmission coefficient will be equal to the plane wave transmission coefficient. This is confirmed by the experimental results such as those shown in Figure 7.

In order to study the effect of the plane wave spectrum on measurements of insertion loss for cases when $T'(\theta)$ is not slowly changing, it is necessary to introduce specific forms for the plane wave spectrum and the transmission coefficient. The complex expression for the transmission coefficient prevents an analytical solution and equation (3) must in general be integrated by numerical means. If the truncated parametric array is considered as a line endfire array then it can be shown [7] that

$$S(\theta) = Q_0[(e^{ikL(1-\cos\theta)} - 1)/ik(1-\cos\theta)] , \qquad (5)$$

where Q_0 is a constant determined by the source strength and L is the length of the array. Substitution of this solution into equation (2) gives

$$A(z) = Q_0\, e^{ikz} \ln[z/(z-L)], \qquad (6)$$

as given in [15]. Evaluation of equation (3) by numerical techniques and normalisation by A(z) enables the effective transmission coefficiet $T'_a(z)$ to be evaluated where

$$T'_a(z) = A_t(z)/A(z). \qquad (7)$$

This is the apparent transmission coefficient that will be measured experimentally with a parametric source and is in general a function of range z. Note that the result does not depend on where the panel is inserted between the acoustic filter and hydrophone.

The effect of the plane wave spectrum on the measured transmission coefficient is illustrated in Figure 8 which shows the measured results for the insertion loss of a 12.7mm thick Perspex (polymethylmethacrylate) panel 0.6 x 0.54m in size over the frequency range 20 to 150kHz. The experimental results are compared with the theoretical predictions for a plane wave and numerical results of equation (7). These calculations were based on data for the velocities and attenuations of Perspex from the literature [16]. As can be seen the results agree with the plane wave predictions for frequencies up to 50kHz and between 70 and 90kHz. However significant deviations from the plane wave result are seen around 55kHz and 107kHz with rapid changes in the loss and a loss of 2.6db greater than predicted at 111kHz. Over the region from 100 to 107kHz the loss is actually negative, so that the signal level is higher at the observation position with the panel present.

The theoretical results of equation (7) are in very good agreement with the experimental observations and show that the plane wave spectrum of the source is responsible for the deviations from the plane wave result. Detailed investigation shows that the deviations do occur where the transmission coefficient changes rapidly with angle for small angles of incidence. Model calculations show that the negative loss occurs because of the way in which the transmission coefficient phase changes with angle of incidence. This changes the phases of the components in the plane wave spectrum in such a way that the source appears to be nearer to the observation position [7].

It should be noted that:

(a) The deviations observed are not specific to the use of a parametric array as a source but can also occur for conventional sources at finite ranges [17].

(b) These deviations decrease with increasing range but may still be of the order of 1dB for a separation of 2.0m.

Oblique Incidence Measurements.

The analysis outlined above can be extended to the case of oblique incidence but with considerably increased complexity. In reference [7] an expression for the apparent transmission coefficient that will be observed at an angle θ_o to the normal when measurements are made with a parametric array is obtained. The result applies when θ_o is not small and shows that the observed transmission coefficient will be a complex average of the plane wave transmission coefficient. In particular the result is very sensitive to phase variations of the transmission coefficient with angle of incidence.

This is best demonstrated by Figure 9 which shows the insertion loss and phase of the transmission coefficient for a 12.1mm thick Perspex panel at 59.6kHz as a function of angle of incidence. It should be noted that the parametric array facility also allows the phase of the transmission coefficent to be determined accurately. In this case the plane wave theory predicts two maxima at angles of 12.5 and 34.8 degrees; the first is a broad peak while the second is narrow with a maximum loss of 32dB. The theoretical predictions of reference [7] show a significantly altered response with the two peaks affected differently. Thus although the plane wave spectrum can be considered to introduce an averaging effect, the result is very dependant on the form of the phase variation of the transmission coefficient with angle.

The experimental data is generally in reasonable agreement with the theoretical predictions with maximum deviations of about 1.8dB and 15 degrees of phase. In fact the data shown has been used to estimate the elastic properties of the sample by optimising the fit of the theory using least squares minimisation. The resulting values for the velocities of sound are in very good agreement with values in the literature although much more work needs to be done on this aspect.

As a final example of the ability of the technique Figure 10 shows the measured insertion loss of a 12.7mm Perspex sheet as a function of frequency for an angle of incidence of 25°. The plane wave theory predicts two loss peaks at 66.3 and 111.8kHz while for the panel insonified by a parametric source the predicted peaks occur at 62.0 and 111.8kHz. It is interesting to note the shift of the lower peak as these peaks are very sensitive indicators of the shear wave velocity. The experimental results are in very good agreement with the improved theory.

The same experimental technique has been used to measure a wide range of materials including glass reinforced plastics and rubbers. The technique may also be used to measure the reflection loss of material samples with the problems due to edge diffraction significantly reduced [6].

BACKSCATTERING MEASUREMENTS

Experimental techniques of measuring backscattering from targets are required to confirm theoretical predictions for objects with a high degree of symmetry and also to measure the response of more complicated shapes for which theoretical predictions are not possible. Here a laboratory technique of measuring backscattering that uses a parametric array as an acoustic source is described. The method utilises the wideband nature of a parametric array to make measurements over a very wide frequency range and is illustrated by measurements on solid spheres.

The theory of scattering of sound by elastic spheres in a fluid is well established and based on the work of Farran and Hickling [18,19]. The backscattered pressure P_R, measured at a range R from a sphere of radius a is given by

$$P_R = (a/2R)\, P_I \exp(ikR)\, f_R(c_1/c, c_2/c, \rho_1/\rho, ka, R/a) \qquad (8)$$

where P_I is the incident plane wave amplitude and k is the angular wavenumber. Here ρ_1, c_1 and c_2 are the density, the compressional and shear wave velocites within the sphere, and ρ and c are the density and sound velocity in the surrounding fluid. The form function f_R describes the monostatic scattering characteristics for a sphere of particular material at a normalised range R/a. For R>>a, i.e. an observation position in the farfield of the sphere, the form function becomes independant of range and equal to the farfield value f_∞. For measurements made at finite range it is, therefore, important to consider the effect of the observation range. Both f_R and f_∞ can be calculated from expressions given by Hickling [19].

The experiments were performed using a similar system to that used to measure the transmission properties of panels (see Figure 11). The technique relied on the stability of the acoustic output to enable the coherent background signal to be subtracted to leave the scattered signal. This was necessary because the hydrophone received the small backscattered wave in the "tail" of the outgoing wave where multipaths were also possible.

The technique is illustrated in Figure 12 which shows the signals that were recorded while making measurements on a stainless steel sphere 19mm in radius with a pulse 25μs long (f_c=40kHz). Initially the signal scattered from the sphere was recorded in the presence of the background signal (a). It should be noted that the time sequence shown starts after the outgoing pulse has finished. The sphere is then removed and the background signal is recorded (b). Subtraction of the background signal leaves the backscattered signal (c) which is due to the insertion of the sphere alone. Finally it was necessary to record the reference pressure waveform at the position of the sphere (d). This was achieved by moving the hydrophone to the appropriate position and rotating the hydrophone through 180° about its vertical axis to ensure that any variation in the hydrophone sensitivity with direction was not important. The form function of the sphere was then obtained from the ratio of the Fourier transforms of the waveforms shown in Figures 4(c) and 4(d).

The resulting backscattered and reference waveforms for a longer pulse of 50μs (f_c=20kHz) are shown in Figure 13 for comparison. For the higher frequency case the waveform contains many multiple pulses due to elastic waves in the sphere that give rise to narrow resonances seen in the form function for ka>5. For the lower frequency case the frequency content of the pulse is below that of the elastic resonances. The low amplitude pulse visible beyond the main pulse can, therefore, be identified as the creeping wave that goes round the back of the sphere and back to the hydrophone.

Figure 14 shows the form function measured for a 19mm radius stainless steel sphere at a range of 0.15m. The results were obtained using three different pulse lengths (55, 25 and 12.5μs) and cover the frequency range 10 to 120kHz. The results for the different pulse lengths are consistent in the regions of overlap and are also in very good agreement with the theoretical predictions over most of the frequency range. The experimental results show both the ripple due to the creeping wave for ka<5 and the pronounced elastic resonances for higher ka values. The positons of these resonances are very sensitive to the elastic wave velocities in the sphere and were used to estimate the velocities used in the numerical calculations. These values were consistent with those in the literature.

Results for a smaller (a=12.7mm) tungsten carbide sphere are shown in Figure 15. In this case the results cover the range from 15kHz to 175kHz. They again show good quantitative agreement at low frequencies although at higher frequencies the measured values are significantly lower than the theoretical predictions. This is attributed to the shadowing effect of the hydrophone which is more significant for smaller targets and higher frequencies. This difference was consistent with measurements of the shadowing effect made with two hydrophones and can be reduced by increasing the observation range.

LABORATORY APPLICATIONS OF PARAMETRIC ACOUSTIC ARRAYS

Two further factors must be considered when comparing the agreement between experiment and theory. Firstly the incident wavefield was not planar but came from an array at a finite range. The effect of this is likely to be similar to that of a finite observation range but not so significant. Secondly, the results were obtained from signals that were truncated by applying windows that were typically 0.5 to 1ms long. This will result in the true spectra being convolved with the transform of the window and will produce some smoothing of rapid changes in the form function.

The use of this technique to measure scattering from solid cylinders and cylindrical shells is currently being investigated with promising initial results. It is intended to extend the technique to make measurements as a function of scattering angle.

CONCLUSION

The results presented show the potential of a parametric array as a versatile tool for laboratory measurements where its wideband frequency ability and small spot size can be very effective.

ACKNOWLEDGEMENT

The author acknowledges the help of Professor H.O. Berktay and many others, past and present, in the School of Physics, University of Bath. Particular thanks go to A.H.A. Moustafa for his assistance with the sphere scattering measurements. The author also acknowledges the support of the Procurement Executive, Ministry of Defence for various parts of this work.

REFERENCES

[1] Westervelt, P.J. (1960). "Parametric end-fire array". J. Acoust. Soc. Amer., 32, 934 (A).

[2] Bellin, J.L.S. and Beyer, R.T. (1962). "Experimental investigation of an end-fire array". J. Acoust. Soc. Amer., 34, 1051-1054.

[3] Bjørnø, L. (1975). "Underwater applications of non-linear ultrasound". *Ultrasonics International 1975 Conference Proceedings*, 238-244.

[4] Konrad, W.A. (1979). "Applications of the parametric source". In: *Proceedings of the Institute of Acoustics Conference on Applications of Non-linear Acoustics*, University of Bath, September 1979.

[5] Humphrey, V.F. (1981). "The measurement of acoustic properties of specimens of limited size by use of a parametric source". *Ultrasonics International '81 Conference Proceedings*, 360-365.

[6] Humphrey, V.F. (1985). "The measurement of acoustic properties of limited size panels by use of a parametric source". J. Sound Vib., 98, 67-81.

[7] Humphrey, V.F. and Berktay, H.O. (1985). "The transmission coefficient of a panel measured with a parametric source". J. Sound Vib., 101, 85-106.

[8] Humphrey, V.F., Murphy, C. and Moustafa, A.H.A. (1987). "Wideband backscattering measurements using a parametric array". *Ultrasonics International '87 Conference Proceedings*, 265-270. Butterworths.

[9] Thorne, P.D. and Pace, N.G. (1984). "Acoustic studies of broadband scattering from a model rough surface". J. Acoust. Soc. Amer., 75, 133-144.

[10] Berktay, H.O. (1965). "Possible exploitation of non-linear acoustics in underwater transmitting applications". J. Sound Vib., 2, 435-461.

[11] Moffet, M.B. and Blue, J.E. (1980). "Hydrophone non-linearity measurements". *N.U.S.C. Technical Memorandum 801150.*

[12] Humphrey, V.F. and Hsu, C.H. (1980). "Non-linearity of cylindrical hydrophones used for the measurement of parametric arrays". In: *Proceedings of the Institute of Acoustics Conference on Transducers for Sonar Applications*, University of Birmingham, December 1980.

[13] Moffet, M.B. and Henriquez, T.A. (1982). "Hydrophone non-linearity measurements". J. Acoust. Soc. Amer., 72, 1-6.

[14] Brekhovskikh, L.M. (1980). *"Waves in Layered Media"*. London: Academic Press, 2nd. Edition.

[15] Berktay, H.O. and Shooter, J.A. (1973). "Nearfield effects in end-fire line arrays". J. Acoust. Soc. Amer., 53 , 550-556.

[16] Read, B.E. and Dean, G.D. (1978). "The Determination of Dynamic Properties of Polymers and Composites". Bristol: Adam Hilger.

[17] Humphrey, V.F. (1986). "The influence of the plane wave spectrum of a source on measurements of the transmission coefficient of a panel". J. Sound Vib., 108 , 261-272.

[18] Faran, J.J. (1951). "Sound scattering by solid cylinders and spheres". J. Acoust. Soc. Amer., 23 , 405-418.

[19] Hickling, R. (1962). "Analysis of echoes from a solid elastic sphere in water". J. Acoust. Soc. Amer., 34 , 1582-1592.

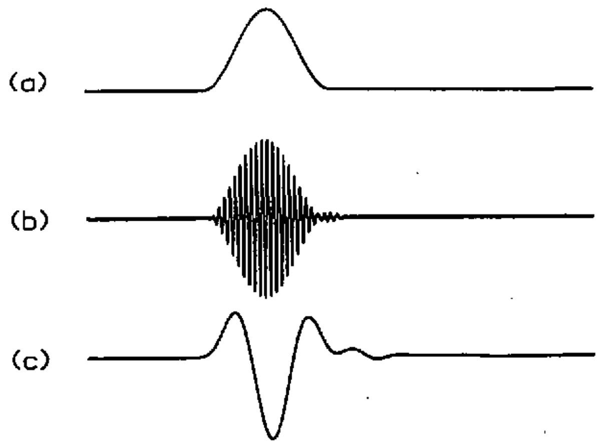

Figure 1. Experimental waveforms. (a) Raised cosine bell envelope (f_c=40kHz); (b) modulated 920kHz carrier signal applied to transducer; (c) resulting parametric array low frequency output. Record length=1ms.

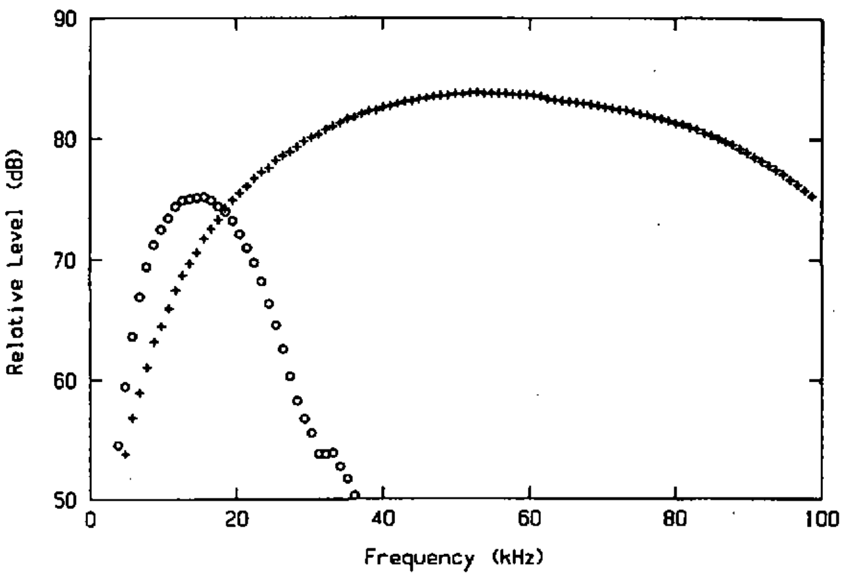

Figure 2. Normalised spectra of low frequency pulses generated by parametric array for different modulation envelopes. +, f_c=40kHz; o, f_c=10kHz.

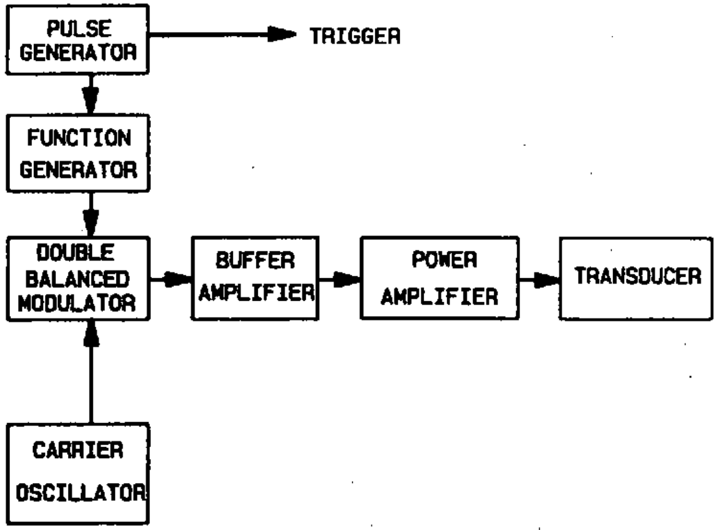

Figure 3. Block diagram of transmitting electronics.

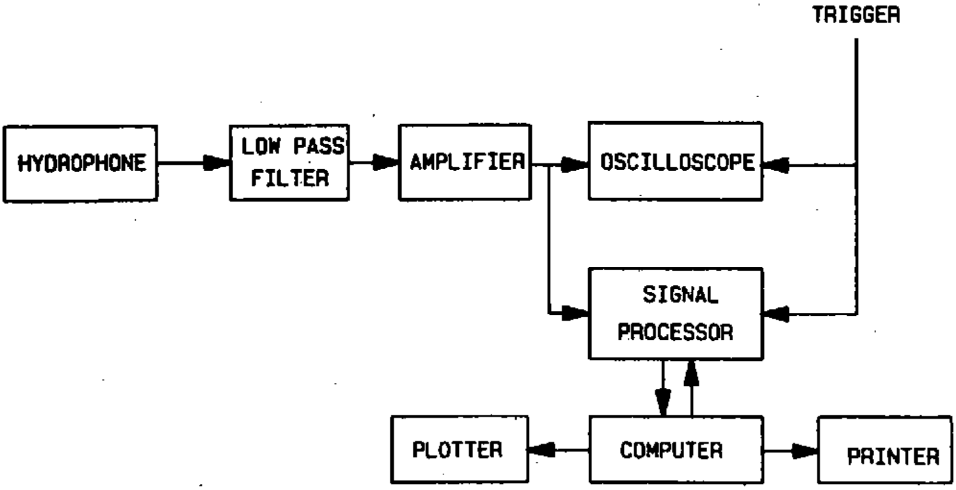

Figure 4. Block diagram of receiving electronics.

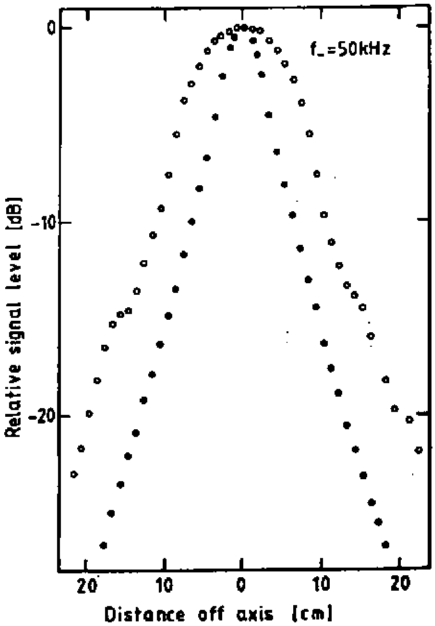

Figure 5. Truncated parametric array beam profiles at 50kHz for L=0.6m. ●, Immediately behind filter; o, R=0.75m.

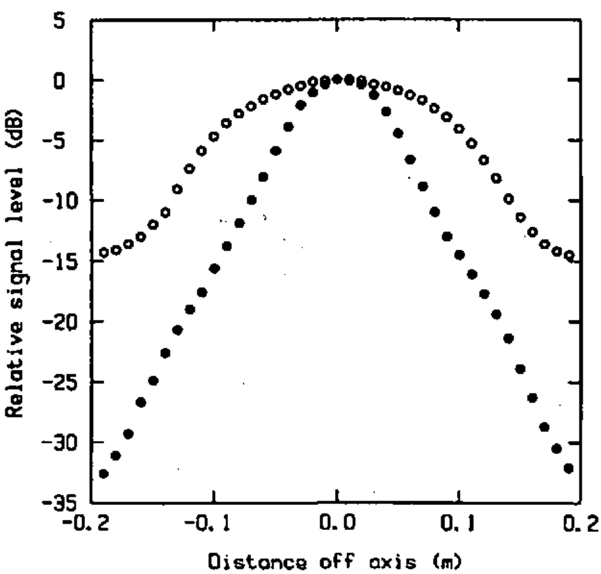

Figure 6. Truncated parametric array beam cross-sections for L=0.56m and R=0.66m. ●, 80kHz; o, 20kHz.

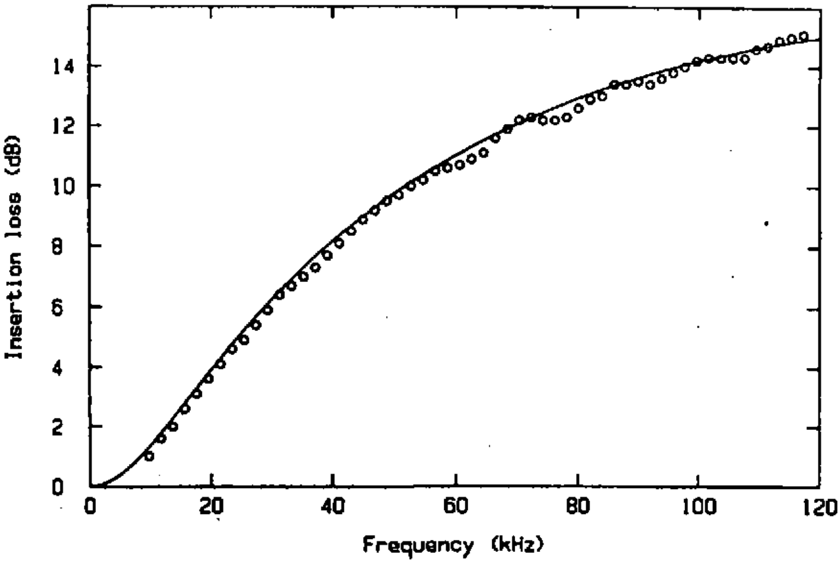

Figure 7. Insertion loss for a 10.7mm thick aluminium plate at normal incidence. o, Experiment; - - -, plane wave theory.

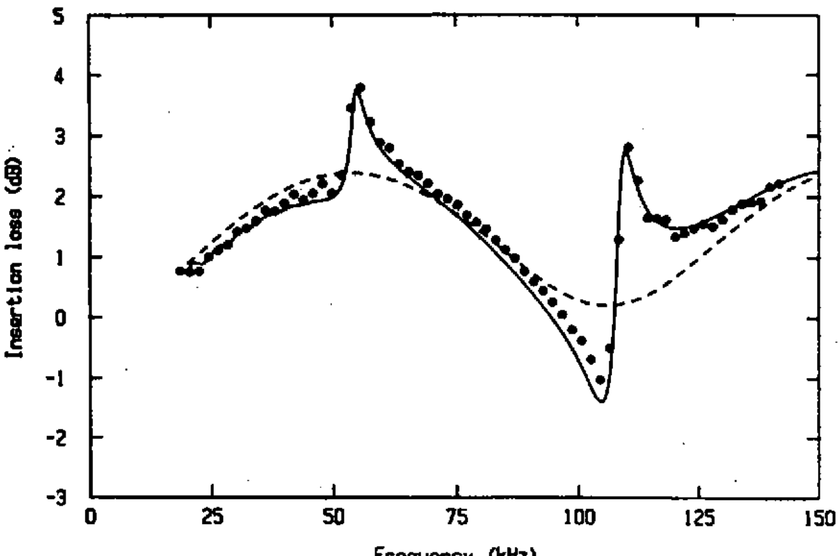

Figure 8. Insertion loss for a 12.7mm thick Perspex panel at normal incidence. •, Experiment; - - -, plane wave theory; ——, theory including effect of plane wave spectrum.

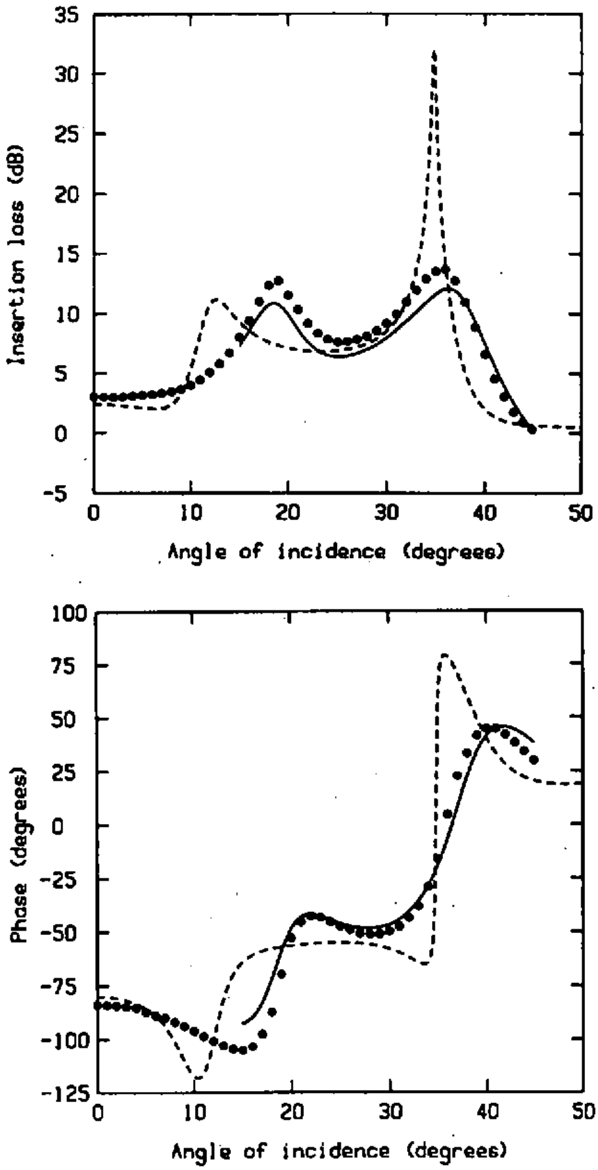

Figure 9. Insertion loss and phase of transmission coefficient vs. angle of incidence for a 12.1mm thick Perspex panel at 59.6kHz. ●, Experiment; - - -, plane wave theory; ——, theory including effect of plane wave spectrum.

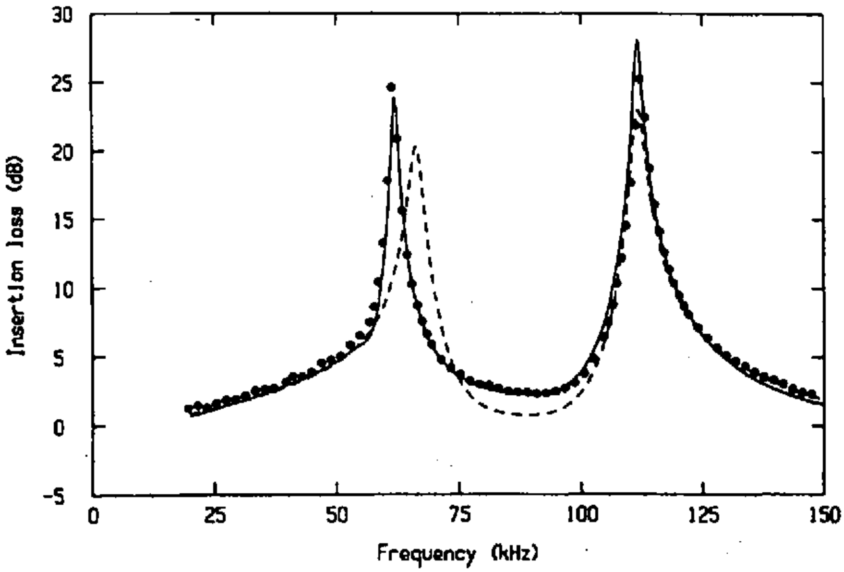

Figure 10. Insertion loss for a 12.7mm thick Perspex panel at 25° angle of incidence. •, Experiment; - - -, plane wave theory; ——, theory including effect of plane wave spectrum.

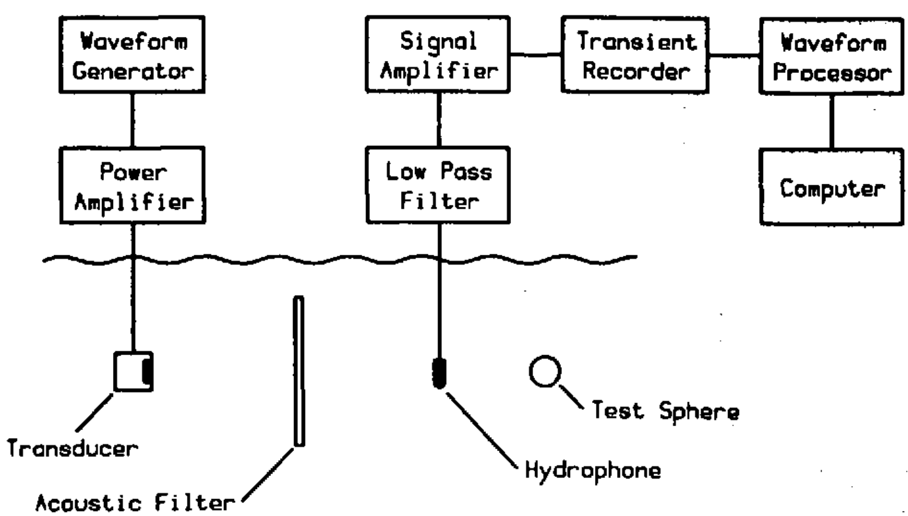

Figure 11. Experimental system for backscattering measurements.

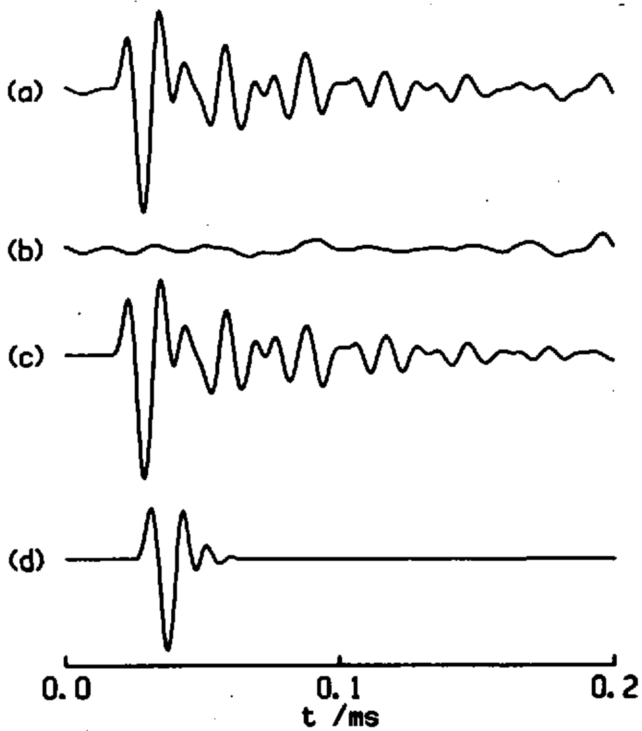

Figure 12. Experimental waveforms for a 20μs pulse. (a) Backscattered plus background; (b) background; (c) backscattered; (d) reference.

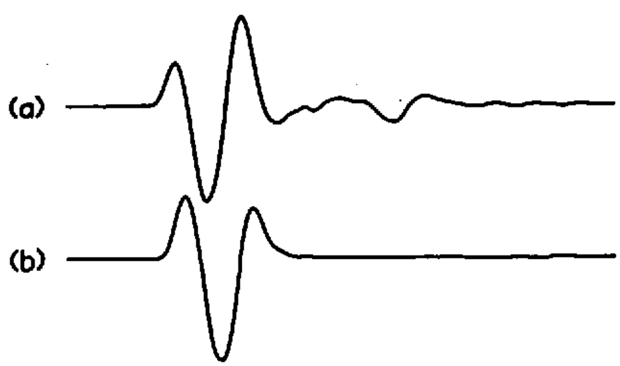

Figure 13. Experimental waveforms for a 40μs pulse. (a) Backscattered; (b) reference.

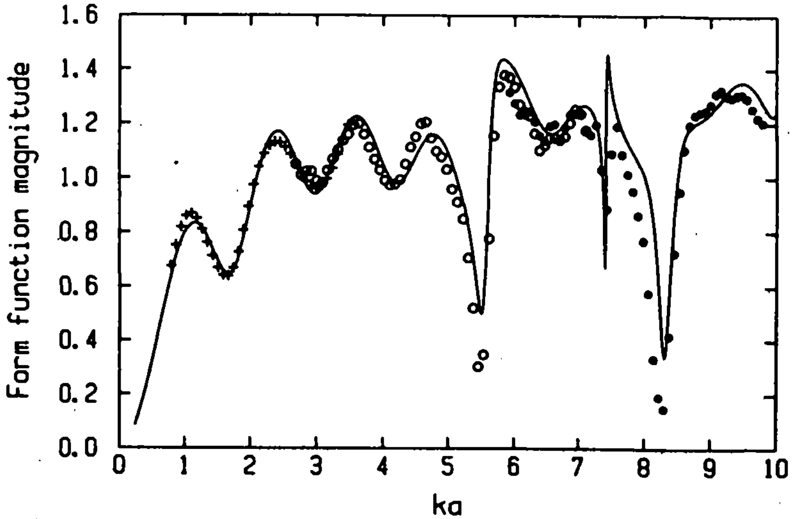

Figure 14. Form function for stainless steel sphere (a = 19mm, R = 0.15m).
- - -, Theory; +, o and • experiment (fc = 17.5, 40 and 80kHz).

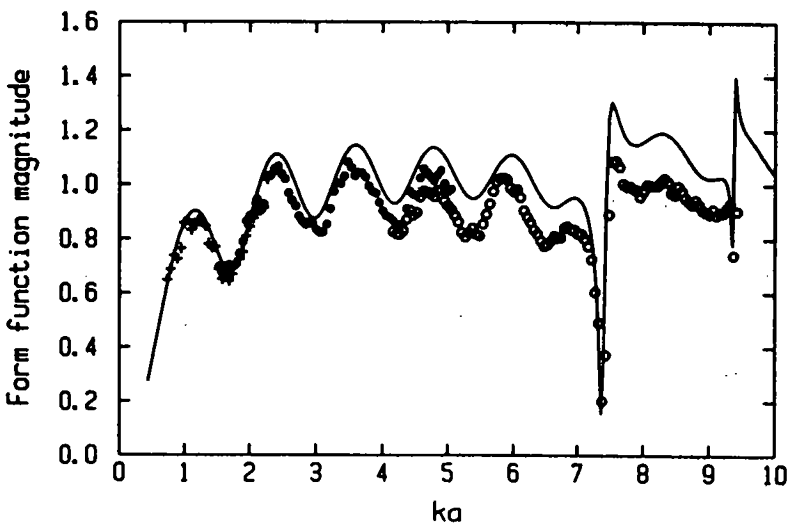

Figure 15. Form function for tungsten carbide sphere (a = 12.7mm, R = 0.1).
- - -, Theory; +, • and o experiment (fc = 17.5, 40 and 80kHz).